OPTOELECTRONICS AND ADVANCED MATERIALS – RAPID COMMUNICATIONS Vol. 1, No. 6, June 2007 p. 281 - 286

Spectroscopic characterization of Sm^{3+} ions in PVA film

A. K. ADIYODI, P. V. JYOTHY, T. F. TONEY, GIJO JOSE, N. V. UNNIKRISHNAN*
School of Pure &Applied Physics, Mahatma Gandhi University, Kottayam-686560, India

Samarium doped Polyvinyl Alcohol (PVA) films were prepared and the optical properties of the films were investigated. By applying Judd-Ofelt theory the Ω parameters were obtained from the absorption spectrum. Various radiative parameters like transition probability for each level (A_J), total transition probability (A_T), branching ratio (β_R), radiative lifetime (τ_R) and absorption cross section (σ_A) were calculated. The theoretically obtained branching ratio and integrated absorption cross section are found to be greater for the transition $^4G_{7/2}$->$^6H_{11/2}$. The emission spectra obtained at 595nm supports the theoretical results with high-stimulated emission cross-section (σ_E) and high optical gain.

(Received March 19, 2007; accepted April 25, 2007)

Keywords: Rare earth, Samarium, Polyvinyl alcohol, Judd-Ofelt Parameters

1. Introduction

Polymers are considered good host materials because they can be designed to yield a variety of bulk physical properties and they normally exhibit long-term stability and possess flexible reprocessability. They can be processed easily, which is an advantage in the fabrication of optical devices [1]. Rare earth ions have been widely used in silica glass based lasers and optical amplifiers. However, in recent years, rare earth ions-containing polymers have attracted much attention for their potential applications for luminescence devices, laser systems and optical communication components [2–5]. Polymers host make it possible to incorporate rare earth ions in higher concentrations preventing concentration quenching at higher concentrations [6]. Further poly vinyl alcohol films can be used as a host matrix for transition metal elements, rare earth ions, dyes, nano particles etc., which can be used for wide range of applications in image storage, holography, laser applications, sensors, display applications, photovoltaic cells etc. [7-10]. In particular photo acoustic studies of Sm^{3+} ions in poly vinyl alcohol have been reported [11]. Upconversion mechanisms are seen in Sm^{3+} ions doped matrices and such a property can be used in storage and other photonic applications. The spectroscopic studies of Sm^{3+} in the polymer PMMA matrix has been reported but such works are relatively limited in PVA matrix. In view of these factors we have attempted spectroscopic studies of Sm^{3+} ions in PVA matrix. The Judd–Ofelt theory has been widely used to estimate the radiative properties of the rare earth containing materials because the model provides reasonable values on average. In this paper, optical properties of samarium ions doped PVA films were studied. The Judd–Ofelt phenomenological parameters, Ω_2, Ω_4 and Ω_6 of doped material were obtained from the absorption spectrum. Based on the Judd–Ofelt theory [12, 13], the transition probabilities, fluorescence branching ratios and radiative lifetime of Sm^{3+} doped PVA films were calculated. The investigation of radiative properties corresponding to the $^4G_{7/2} \rightarrow {}^6H_{11/2}$ transition indicated that it is a laser transition.

2. Experimental

Three samples A, B and C with Samarium (1%, 3%, 5% by weight) respectively doped in polyvinyl alcohol (PVA) films were grown by slow evaporation at room temperature [14]. PVA was dissolved in double-distilled water and then heated on a hot plate for a few minutes. Subsequently the Samarium Chloride is dissolved in water were mixed with the PVA solution. Following the procedure reported elsewhere Sm^{3+}ions were added in their chloride form in solutions and it has been understood that the added amount would be intact in the matrix [15-17]. The solution cast into a polypropylene dish and was kept at 50 °C for two days. The films were peeled off from the polypropylene dish. These films were used for spectral investigations. The thickness of the films were measured using Prism Coupler (Metricon 2010) at 633nm and were found to be 17 μm. The refractive index was also measured and the values were found to be 1.49. The absorption and fluorescence spectra were recorded using the spectrophotometers Shimadzu –UVPC 2401 and Shimadzu-RFPC-5301 respectively.

3. Theoretical analysis

The theory of atomic spectra allows identification of definite J levels of $4f^5$ in the Sm^{3+} ion. A convenient way of representing the intensity of an absorption band is to measure the oscillator strength of the transition, which is found to be proportional to the area under the absorption line shapes. The oscillator strength (f) can be expressed in terms of the molar extinction coefficient (ε), and the energy of the transition in wave number (ν) by the relation [18].

$$f_{exp} = 4.32 \times 10^{-9} \int \varepsilon(\nu) d\nu \qquad (1)$$

The absorption properties of rare earth ions are best distinguished in the context of Judd-Ofelt theory [19]. In essence the 4f→4f transitions of a rare earth ion can be described as a simple linear combination of the so-called J-O parameters Ω_λ (λ=2, 4, 6). The coefficients of each linear combination of Ω_λ are independent of the host and are determined by the fundamental nature of the 4f wave functions and the particular transitions at hand.

According to J-O theory

$$f_{ed} = \frac{\nu}{(2J+1)} \left[\frac{8\pi^2 mc}{3h} \frac{(n^2+2)^2}{9n} \right] \sum_{\lambda=2,4,6} \Omega_\lambda \left\langle \psi J \middle\| U^\lambda \middle\| \psi' J' \right\rangle^2 \qquad (2)$$

where (2J+1) is the degeneracy of the ground state, ν is the mean energy of the $\left|\psi J\right\rangle \rightarrow \left|\psi' J'\right\rangle$ transition, U^λ is a unit tensor operator of rank λ and Ω_λ's are known as J-O intensity parameters. Because of the electrostatic shielding of the 4f electrons by the closed 5p shell electrons the matrix elements of the unit tensor operator between two energy manifolds in a given rare earth ion do not vary significantly when it is incorporated in different hosts. Therefore, the matrix element computed for the free ion may be used for further calculations in different media and are reported by Carnall et al. [19]. In order to obtain the accuracy of the intensity parameters obtained, the root-mean-squared deviations (δ_{rms}) are calculated using the relation $\delta_{rms} = \Sigma \left[\frac{(f_{exp} - f_{cal})^2}{N-M} \right]^{\left(\frac{1}{2}\right)}$, where N is the number of levels fitted and M is the number of parameters determined. The bonding parameter (δ) defined as $\delta = \left[(1-\overline{\beta}) / \overline{\beta} \right] \times 100$ where $\overline{\beta} = \sum_N \beta / N$ and $\beta = \nu_c / \nu_a$ (the nephelauxetic ratio), ν_c and ν_a are the energies of the corresponding transitions in the complex and aqua ion respectively, and N refers to the number of levels used to compute $\overline{\beta}$ values. Depending upon the environmental field, δ may be positive or negative indicating covalent or ionic bonding respectively [18].

Radiative transition parameters such as total radiative transition probability (A_T), radiative lifetime (τ_{RAD}), and the fluorescence branching ratio (β_R) are calculated using the known expressions [18]. The position of J levels of $4f^n$ in condensed matter is treated by the same techniques as for monatomic entities, but the probabilities of absorption and emission between J levels are entirely different. Radiative transition probabilities of the rare earths in polymers are composed mainly of the electric dipole contribution and to a much lesser extent by the magnetic dipole contribution. For rare-earth ions, taking account of multiple terms splitting, its spontaneous radiative transition probability becomes

$$A^{ed}{}_{JJ} = \frac{64\pi^2 e^2 \upsilon^3}{3h(2J+1)} \left[\frac{n(n^2+2)^2}{9} \right] S_{ed} \qquad (3)$$

where $S_{ed} = \sum_{\lambda=2,4,6} \Omega_\lambda \left\langle \psi J \middle\| U^\lambda \middle\| \psi' J' \right\rangle^2 \qquad (4)$

As the coefficients for spontaneous emission equal the reciprocal radiative relaxation time, we have

$$A^{ed}{}_{JJ} = \tau^{-1}{}_{Rad} \qquad (5)$$

$$\text{or} \qquad \tau_{rad} = \frac{1}{\sum_{J'} A_{JJ'}} \qquad (6)$$

The position of the lines in absorption or emission spectra seems to be independent of the surroundings. Their intensity ratios vary strongly, indicating certain selection rules, which are reflected by the branching ratio. The relative amplitudes of the fluorescence transitions or fluorescence branching ratio is given by

$$\beta_{JJ'} = \frac{A_{JJ'}}{\sum_{J'} AJJ'} \qquad (7)$$

Branching ratio is the ratio of the radiative transition probability to the total radiative relaxation rate. It measures the percentage of emission for a given transition from a state with respect to all other transitions from this state. The integrated absorption cross-section or effective cross-section (σ_a) for stimulated emission is estimated using the Fuchtbauer–Landenberg equation.

$$\sigma_a = \frac{A(\psi J)}{8\pi c n^2 \upsilon^2} \qquad (8)$$

The effective cross-section which is the stimulated cross-section integrated over the total band gives a measure of the peak stimulated emission cross-section for transitions under the assumption that the bands do not contain sharp emission peaks. Knowing the radiative transition probability and effective fluorescence line width the stimulated emission crossection (σ_E) can be calculated using the equation

$$\sigma_E = \frac{\lambda_p{}^4}{8\pi c n^2 \Delta\lambda_{eff}} A(\psi J, \psi' J') \qquad (9)$$

where λ_p is the peak wavelength of the emission transition and $\Delta\lambda_{eff}$ is the effective band width of the emission transition.

4. Results and discussion

PVA films are highly transparent in the visible range of wavelength which may be utilized in transparent electronic devices. The thermal property of the PVA film was obtained using

TGA analysis. It was found that the degradation of the PVA film starts at around 300 °C (Fig. 1). The degradation of polymers starts with free radical formations at weak bonds and/or chain ends, followed by their transfer to adjacent chains via interchain reactions.

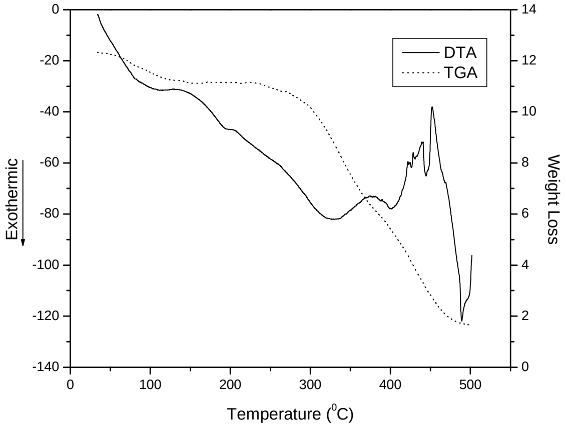

Fig. 1. TGA/DTA curve of PVA.

The major mechanism for transitions in rare earth ions is induced electric dipole arising from the very weak mixing of the order of magnitude of the ground state $4f^n$ wave function with functions of the opposite parity. The absorption spectra of doped PVA for different wt% of Samarium ions follow a linear relationship with Sm^{3+} concentration. The ground state of the Sm^{3+} ion is $^6H_{5/2}$ and the absorption bands arise due to transitions from this level to various excited levels. The spectral lines observed are assigned for different excited states $^4G_{7/2}$, $^4H_{9/2}$, $^4D_{3/2}$, $^6P_{7/2}$, $^6P_{3/2}$, $^6P_{5/2}$, $^4G_{9/2}$, $^6I_{13/2}$, $^6I_{11/2}$, [19] and is given in Fig. 2.

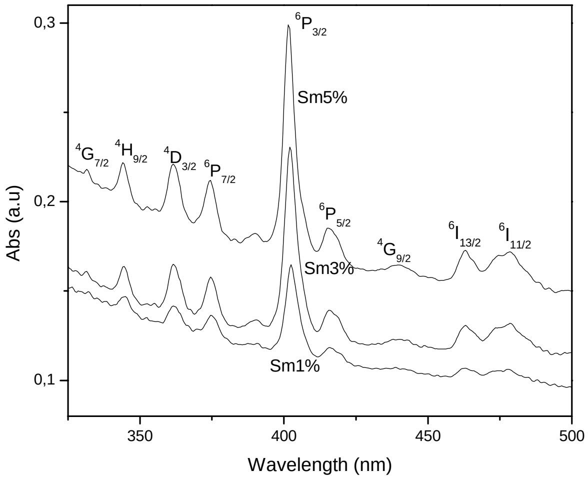

Fig. 2. Absorption spectra of Samarium in PVA at different concentrations.

For most practical purposes the oscillator strengths and the connected radiative transition probabilities obtained from the absorption spectra correspond to some average values due to the total number of sites. A small shift of the free ion levels to lower energies can be observed as a result of the covalency between the rare earth and the polymer matrix. Experimentally determined oscillator strengths and the calculated oscillator strengths are tabulated in Table 1.

Table 1. The rms deviations for the oscillators strengths.

Transition from $^6H_{5/2}$	Sm1%			Sm 3%			Sm 5%		
	f_{mea} 10^{-6}	f_{cal} 10^{-6}	δ_{rms} 10^{-6}	f_{mea}	f_{cal} 10^{-6}	δ_{rms} 10^{-6}	f_{mea} 10^{-6}	f_{cal} 10^{-6}	δ_{rms} 10^{-6}
$^4H_{9/2}$	0.17	0.08	0.19	0.29	0.18	0.4025	0.27	0.21	0.41
$^4D_{3/2}$	0.17	0.26		0.46	0.57		0.61	0.66	
$^4P_{7/2}$	0.23	0.27		0.51	0.63		0.52	0.66	
$^4P_{3/2}$	1.14	1.12		2.43	2.41		2.79	2.78	
$^6P_{5/2}$	0.14	0.17		0.36	0.36		0.42	0.42	
$^4I_{13/2}$	0.11	0.08		0.25	0.18		0.31	0.20	
$^4I_{11/2}$	0.19	0.009		0.58	0.02		0.66	0.02	

The root mean square deviations in determining oscillator strength are also given in Table 1 and these values are comparable with other Sm^{3+} systems [20, 21]. The measured and calculated values of electric dipole strengths for different absorption levels are tabulated in Table 2. The J-O parameters of Sm^{3+} in PVA matrices for the three samples are given in Table 3.

Table 2. Electrical dipole strength for different absorption levels.

Transition from $^6H_{5/2}$	Sm 1%		Sm 3%		Sm 5%	
	$S_{meas}\times10^{-22}$	$S_{cal}\times10^{-22}$	$S_{meas}\times10^{-22}$	$S_{cal}\times10^{-22}$	$S_{meas}\times10^{-22}$	$S_{cal}\times10^{-22}$
$^4H_{9/2}$	0.42	0.20	0.72	0.45	0.66	0.53
$^4D_{3/2}$	0.45	0.67	1.19	1.46	1.56	1.69
$^4P_{7/2}$	0.60	0.71	1.35	1.67	1.37	1.77
$^4P_{3/2}$	3.26	3.22	6.93	6.89	7.95	7.94
$^6P_{5/2}$	0.43	0.50	1.06	1.07	1.24	1.24
$^4I_{13/2}$	0.36	0.26	0.83	0.61	1.01	0.65
$^4I_{11/2}$	0.64	0.09	1.97	0.23	2.25	0.22

Table 3. The Judd-Ofelt parameters of Sm^{3+} in PVA matrices.

Sample	JO parameters (10^{-20} cm^2)			Q- factor	Order	Bonding parameter
	Ω_2	Ω_4	Ω_6			
Sm1%	19.85	0.19	0.09	2.08	$\Omega_2>\Omega_4>\Omega_6$	0.29
Sm3%	43.63	0.41	0.21	1.91	$\Omega_2>\Omega_4>\Omega_6$	0.27
Sm5%	50.77	0.47	0.22	2.08	$\Omega_2>\Omega_4>\Omega_6$	0.21

and the value is found to be greater for Sm 5% sample. It has been well established that as the concentration of the rare earth ions increases in a matrix, the structural network gets modified with the result that the covalent bonding increases. The parameter has a direct relationship with the structural network which is reflected in the Ω_2 values [22]. The increase in covalency (R-O covalency) is manifested directly in the increase of the J-O parameter [23]. These parameters in turn determine the electric dipole and magnetic dipole line strengths of a transition. The J-O parameters are functions of crystal field parameters, intraconfigurational radial integral and energy separation of the $4f^N$ and opposite parity configuration. Hence these parameters are dependent on the oscillator strengths and are found to vary from site to site. The bonding parameter (δ) obtained are also given in Table 3 and found to be positive which indicates the presence of covalent bonds.

Jorgensen and Reisfeld [24] related the intensity parameters Ω_4 and Ω_6 to the rigidity of various hosts such as crystals, glasses, solutions and vapours. Takebe et al. [25] suggested that the ionic packing ratio is related to the spontaneous emission probabilities which are determined by the intensity parameters Ω_4 and Ω_6 and it correlates with the rigidity of the polymer hosts and the covalency of the rare earth ion sites. The parameter Ω_2 is related to the covalency and/or structural changes in the vicinity of the Sm^{3+} ion (short range effect) and Ω_4 are related to the long range effects. Covalent bonding has the effect of lowering the electronic levels of the free ion due to the nephelauxetic effect and the value of Ω_2 gets strongly enhanced. A large value of Ω_2 intensity parameter is an indication of high covalence of the metal- ligand bonds and the values are found to be greater in PVA films than in inorganic glasses and aquous solution. High covalent bonding provides greater Ω_2 values, which indicates lower symmetry around the rare earth ion in the host.

According to the Judd-Ofelt theory the JO parameters and spontaneous emission probability are affected by the structural change around rare earth ions and/or the covalency of the rare earth sites [26]. Especially, the spontaneous emission probability which is determined by the value of the Ω_4 and Ω_6 are affected by the covalency of the rare earth ion sites.

Now once the Ω_λ quantities have been determined, they can subsequently be utilized to calculate the properties of fluorescent transitions from $^4G_{5/2}$, $^4G_{7/2}$, and $^4F_{3/2}$ levels that have not been experimentally measured, including the radiative lifetime. The values of the radiative transition probability (A), total radiative transition probability (A_T), radiative life time (τ) fluorescence branching ratio (β_R) and the integrated absorption cross-section for stimulated emission are given in Table 4.

Table 4. The transitions from $^4G_{7/2}$ and their characterization.

Transition from $^4G_{7/2}$	Energy ν cm^{-1}	S_{ed} (10^{-22})	A s^{-1}	A_T s^{-1}	τ_{rad} μs	β(%)	σ_A (10^{-20}cm^2)
$^4G_{5/2}$	2244	9.62	0.41	917.41	1090	0.04	4.67
$^6F_{11/2}$	9095	5.08	7.21			0.78	5.01
$^6F_{9/2}$	10594	3.07	8.25			0.89	4.22
$^6F_{7/2}$	11881	40.63	192.73			20.96	78.42
$^6F_{5/2}$	12737	2.64	20.59			2.23	7.28
$^6F_{3/2}$	13260	12.74	168.09			18.28	54.91
$^6H_{15/2}$	13335	0.01	0.04			0.005	0.01
$^6H_{13/2}$	14822	0.31	1.66			0.18	0.43
$^6H_{11/2}$	16494	57.95	490.60			53.34	103.53
$^6H_{9/2}$	17640	1.07	13.33			1.45	2.46
$^6H_{7/2}$	18891	0.76	14.66			1.59	2.36

The emission spectra of the three samples are given in Fig. 3.

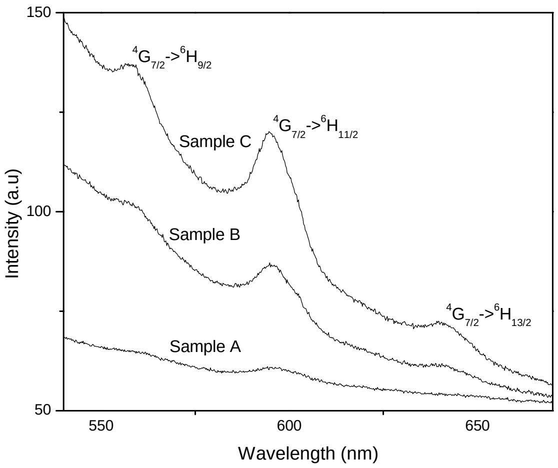

Fig. 3. Emission spectra of the samples.

The main peak is at 595 nm, similar to Sm^{3+} ions. The main peak due to Sm^{2+} ions is at around 700 nm [27-29]. Therefore the appearance of emission spectra due to Sm^{2+} ion is ruled out. From the emission spectra, branching ratio for each level is calculated using the standard procedure [30]. Using the relation (9) the stimulated emission cross section for the levels is calculated. These values are tabulated in Table 5.

Table 5. Cross-section values for the levels of stimulated emission.

Transition	λ_P (nm)	$\Delta\lambda_{eff}$ (nm)	β(%)	σ_e (cm^2)
$^4G_{7/2}\rightarrow{}^6H_{9/2}$	559	11	22.34	6.79×10^{-23}
$^4G_{7/2}\rightarrow{}^6H_{11/2}$	595	12.7	65.54	2.9×10^{-21}
$^4G_{7/2}\rightarrow{}^6H_{13/2}$	642	13.49	11.99	1.2×10^{-23}

From the table it is clear that the transition $^4G_{7/2}\rightarrow{}^6H_{11/2}$ shows the highest stimulated emission cross-section and hence it has high optical gain. This is in agreement with the theoretical obtained branching ratio and integrated absorption cross section for the transition $^4G_{7/2}\rightarrow{}^6H_{11/2}$. The branching ratio and integrated absorption crossection are higher for the transition $^4G_{7/2}\rightarrow{}^6H_{11/2}$ in PVA films than in Zinc Borosulphate (ZnBS) glasses (β=4.4, σ_A=2.5×10^{-20} cm^2) [21]. In alkali flouroborate glasses this transition has a higher value of branching ratio (β=67) and can be used for optical amplification [31]. Hence we can conclude that the transition $^4G_{7/2}\rightarrow{}^6H_{11/2}$ can be utilized for optical amplification in Sm^{3+} doped PVA films. Some of the major advantages attributed to polymers in the context of polymers doped with rare earth ions are (i) the rare earth ions doped polymer matrix shows higher covalent bonding, (ii) such systems are ideal candidates for optical image storage, (iii) a hologram could be written easily at a wavelength corresponding to the absorption peaks of the rare earth ions and (iv) they can be processed easily and exhibit better long term photostability.

5. Conclusion

The optical properties of Sm^{3+} doped PVA films were studied. The various important spectral parameters were obtained from the absorption spectrum such as radiative lifetime, transition probability, branching ratio and absorption cross-sectionn. The transition $^4G_{7/2} \rightarrow {}^6H_{11/2}$ has been identified as the one which yields the maximum flouresence emission. The evaluation of the radiative properties indicate that Sm^{3+} doped PVA is promising for making polymer optical active devices.

References

[1] H. Ma, A. K.Y. Jen, L. R. Dalton, Adv. Mater. **14,** 1339 (2002).

[2] C. Koeppen, S. Yamada, G. Jiang, A. F. Garito, L. R. Dalton, J. Opt. Soc. Am. B **14,** 155 (1997).

[3] K. Kuriki, Y. Koike, Y. Okamoto, Chem. Rev. **102,** 2347 (2002).

[4] H. Liang, Q. Zhang, Z. Zheng, H. Ming, Z. Li, J. Xie, B. Chen, H. Zhao, Opt. Lett. **29,** 1895 (2004).

[5] L. H. Slooff, M. J. A. de Dood, A. van Blaaderen, A. Polman, Appl. Phys. Lett. **76,** 3682 (2000).

[6] T. Kobayashi, K. Kurki, N. Imai, T. Tamura, K. Sasaki, Y. Koike, Y. Okamoto, Proc. SPIE**, 206**, 3623 (1999).

[7] R. Changkakoti, G. Manivannan, A. Singh, R. A. Lessard. Opt. Eng. **32**, 2240 (1993).

[8] Seong-Shan Yap, Wee Ong Siew, Teck Yong Tou, Seik Weng Ng, Applied Optics **41,** 1725 (2002).

[9] J. Thomas, G. A. Kumar, N. V. Unnikrishnan, V. P. N. Nampoori, C. P. G. Vllabhan, Mat.lett. **44,** 275 (2000).

[10] Karthikeyan, Physica B **364,** 328 (2005).

[11] Mithleshkumar, A. R. Dhobale, Mukeshkumar, M. D. Sastry, J. Pol. Sci Part B, Polymer Physics **35,** 187 (1997).

[12] B. R. Judd, Phys. Rev. **127,** 750 (1962).

[13] G. S. Ofelt, J. Chem. Phys. **37**, 511 (1962).

[14] M. Soliman Selim, R. Seoudi, A. A. Shabak, Mater. Lett. **59,** 2650 (2005).

[15] Xianping Fan, Minquan Wang, Guohong Xiong, Mater Sci &Eng. **B21,** 55 (1993).

[16] M. Nogami, T Nagakura, T Hayakawa, Phys. Cond. Matter. **11,** 335 (1999).

[17] M. Nogami, T Nagakura, T Hayakawa, T. Sakai, Chem Mater. **10,** 3991 (1998).

[18] Gijo Jose, Vinoy Thomas, Toney Teddy Fernandez, Amrutha K. Adiyodi, Cyriac Joseph, M. A. Ttyachan, N. V. Unnikrishnan, Physica B **357**, 270 (2005).

[19] W. T. Carnaal, P. R. Fields, K. Rajnak, J. Chem. Phys., **49,** 4424 (1968).

[20] Hao Liang Zhiqiang Zheng, Qijin Zhang, Hai Ming, Biao Chen, Phys. Stat. Sol. (b), **5,** 1149 (2004).

[21] C. K. Jayasankar, E. Rukmini, Optical Materials**, 8,** 193 (1997).

[22] Carnall in Handbook on the Physics and Chemistry of Rare Earths Vol. 3, eds K.A Gschneidner Jr and L. Eyring.

[23] M. B. Saisudha, J. Ramakrishna Phys. Rev. B**, 53,** 6186 (1996).

[24] C. K. Jorgensen, R. Reisfeld, J. Less. Common. Met., **93,** 107 (1983).

[25] H. Takabe, M. Keji, T. Izumitani, J. Non-Cryst. Solids, **178,** 58 (1994).

[26] S. Tanabe, T. Ohyagi, N. Soga, T. Hanada, Phys. Rev. B, **46,** 3305 (1992).

[27] P. P. Sorokon, M. J. Stevenson, J. R. Lankard, G. D. Pettit, Phys. Rev. **127,** 503 (1962).

[28] Butement, F. D. S. Trans. Faraday Soc. **44,** 617 (1948).

[29] G. H. Dieke, R. Sarup, J. Chem. Phys**. 36,** 371 (1962).

[30] R. A. Velapoldi, Phys. Chem. Glasses **14,** 101 (1973).

[31] R. R. Reddy etal Ind. J Pure &Appl Phy. **40,** 577 (2002).

[•] Corresponding author: nvu50@yahoo.co.in.